

AD-A200 940

AD-A200 940

UNLIMITED



RSRE
MEMORANDUM No. 4191

**ROYAL SIGNALS & RADAR
ESTABLISHMENT**

**EXPERIMENTAL MEASUREMENTS OF SCATTERING
FROM SIMPLE WAVELENGTH SIZED PHASE OBJECTS**

Authors: D L Jordan, E Jakeman, R C Hollins

PROCUREMENT EXECUTIVE,
MINISTRY OF DEFENCE,
RSRE MALVERN,
WORCS.

DTIC
ELECTE
NOV 29 1988
S D
C/E

RSRE MEMORANDUM No. 4191

UNLIMITED

88 11 28 292

ROYAL SIGNALS AND RADAR ESTABLISHMENT

Memorandum 4191

TITLE: EXPERIMENTAL MEASUREMENTS OF SCATTERING FROM
SIMPLE WAVELENGTH SIZED PHASE OBJECTS

AUTHOR: D L Jordan, E Jakeman, R C Hollins

DATE: August 1988

SUMMARY

Experimental results are presented for the angular distribution of radiation scattered from single deep grooves etched in silicon. Both visible and infrared radiation is used. Whereas the grooves are wide compared to the wavelength of the visible radiation, they span a range of sizes from approximately twice down to half the infrared wavelength.

Accession For	
NTIS GRA&I	<input checked="checked" type="checkbox"/>
DTIC TAB	<input type="checkbox"/>
Unannounced	<input type="checkbox"/>
Justification	
By	
Distribution/	
Availability Codes	
Dist	Avail and/or Special
A-1	



Copyright
©
Controller HMSO London
1988

RSRE MEMORANDUM NO 4191

EXPERIMENTAL MEASUREMENTS OF SCATTERING FROM SIMPLE WAVELENGTH
SIZED PHASE OBJECTS

D L Jordan, E Jakeman, R C Hollins

LIST OF CONTENTS

- 1 Introduction
- 2 Theory
- 3 Experiment
- 4 Discussion
- 5 Conclusions
- Acknowledgements
- References

LIST OF FIGURES

- 1 Scattering geometry
- 2a Limit of single scattering
- 2b Multiple scattering
- 3 Experimental arrangement
- 4 Angular scans. Upper trace - $\frac{1}{4}$ hour etch, Lower trace - $\frac{1}{2}$ hour etch
- 5a Measured versus predicted angular positions of diffraction minima due to groove width. X - $23.5 \mu\text{m}$ width groove, O - $7.3 \mu\text{m}$ width groove.
- 5b Depth of grooves determined from depth induced diffraction minima versus those determined from profile measurements. Nominal width $20 \mu\text{m}$.
- 6 Schematic diagram showing polarisation planes for infrared measurements
- 7 Angular scan from $30 \mu\text{m}$ deep groove using CO_2 laser
- 8a CO_2 integrated scattering signal versus groove width with incident radiation p-polarised
- 8b CO_2 integrated scattering signal versus groove width with incident radiation s-polarised
- 9 Ratio of CO_2 integrated intensity with incident radiation p-polarised to that with it s-polarised as a function of groove width

1 INTRODUCTION

Scattering of electromagnetic radiation from objects whose dimensions are comparable to, or smaller than the wavelength of the probing radiation is of fundamental importance in many problems involving the scattering of radiation. It is generally thought that conventional physical optics is inappropriate for dealing with objects having dimensions smaller than the wavelength. In this Memorandum we report some measurements of scattering of visible and infrared laser radiation from objects ranging in size from somewhat above to somewhat below the infrared probing wavelength. In particular we concentrate on phase rather than amplitude objects because of their relevance to a wide range of applications such as optical remote surface measurement⁽¹⁾, semiconductor integrated circuit inspection and radar scattering.

For simplicity we have chosen a single groove as the target. A series of silicon slices have been prepared, each slice containing a series of etched equal depth grooves with nominal widths ranging from $4 \mu\text{m}$ to $25 \mu\text{m}$. Each groove, which was 2.5 mm long had a $100 \mu\text{m}$ width groove perpendicular to it near either end to delineate it. In all, four slices were used, having etching times of $\frac{1}{4}$ hour, $\frac{1}{2}$ hour, 1 hour and $1\frac{1}{2}$ hours;

these correspond to depths ranging from 4 μm to 30 μm . When illuminated by CO_2 laser radiation of wavelength 10.6 μm the silicon grooves allow the study of structures ranging from about twice to slightly less than half the wavelength to be conducted. We first briefly outline the elementary physical optics theory for structures large compared to the probing wavelength and then present some measurements of scattering from the grooves using He-Ne laser light. For this case even the smallest groove (4 μm) is many times the probing wavelength (0.63 μm) and so the derived theory should apply. We then present some measurements made using a CO_2 laser. In this case significant differences occur depending on whether the input laser radiation is polarised parallel or orthogonal to the groove direction.

2 THEORY

The situation considered is that shown in Figure 1. A Gaussian profiled beam of width W is incident on the groove of width s and depth d ; for simplicity normal incidence is assumed. The incident radiation is diffracted at the top of the groove, reflected from the bottom and observed in the Fraunhofer region at an angle θ . The neglect of secondary diffraction at the bottom of the groove is justified when

$$\frac{ks^2 \cos \theta}{2d} \gg 1$$

ie when the bottom of the groove is in the Fresnel region of the diffraction pattern produced by the top of the groove. The phase difference corresponding to the path difference between rays AE and ABF is $2\varphi_0 \cos \theta$ where $\varphi_0 = kd$ and $k = 2\pi/\lambda$. Neglecting side wall effects the amplitude A in the far-field direction θ is given by:

$$BF(\theta) \left\{ \int_{-\infty}^{S/2} \exp \left[-\frac{x^2}{W^2} \right] \exp(ikx \sin \theta) dx + \int_{-S/2}^{S/2} \exp \left[-\frac{x^2}{W^2} \right] \exp i(kx \sin \theta + 2\varphi_0 \cos \theta) dx + \int_{-S/2}^{\infty} \exp \left[-\frac{x^2}{W^2} \right] \exp(ikx \sin \theta) dx \right\} \quad (1)$$

where B is a complex constant and $F(\theta)$ is an angle dependent term⁽²⁾ which is unity for normal incidence. The expression given in (1) can be reduced to two integrals, the first of which is the specular term and reduces to a narrow gaussian. When $s \ll W$ the second integral reduces to the product of two terms, one of which is the amplitude variation due to the finite depth of the groove and the other the effect due to the finite groove width. The intensity (AA^*) of the non-specular component is proportional to:

$$2s^2 (1 - \cos(2\varphi_0 \cos \theta)) \frac{\sin^2 \left[\frac{ks \sin \theta}{2} \right]}{\left[\frac{ks \sin \theta}{2} \right]^2} \quad (2)$$

Therefore nulls occur due to the width of the groove in directions ν_n given by

$$\theta_n = \sin^{-1} \left[\frac{n\lambda}{s} \right] \quad ; \quad n = 0, 1, 2 \dots \quad (3)$$

Nulls also occur due to the finite depth of the groove, and occur when

$$2\varphi_0 \cos \theta = 2\pi m \quad ; \quad m = 0, 1, 2 \dots \quad (4)$$

Unlike the width term, the depth induced nulls are equally spaced in $\cos \theta$, the separation between successive minima being $\lambda/2d$. If the angle of incidence is not zero but rather θ_i , then the position of the width induced minima is changed to

$$\sin \theta_n = \frac{n\lambda}{s} + \sin \theta_i \quad (5)$$

The separation between the depth induced minima remains as $\lambda/2d$.

Actually the simple result⁽¹⁾ given here is also correct in the presence of multiple scattering at the groove side walls. Figure 2a shows the limit of single scattering. Wave ABC just escapes the groove with a single scattering (at B). The simplest multiple scattering situation is shown in Figure 2b. Ray ABCD undergoes one extra scattering compared with the situation shown in Figure 2a. Since however $AB = BE$ the situation is equivalent to a single scattering by ray EBCD and the previous arguments apply. A similar result can be shown to apply for all higher multiple scattering situations.

3 EXPERIMENT

The experimental arrangement was as shown in Figure 3. The output from a He-Ne laser was chopped at ~ 500 Hz before impinging on the silicon slice, the angle of incidence being 5.6° . For some of the measurements a lens was used to focus the radiation on the silicon groove to increase the measured signal-to-noise ratio. The detector was a 10 mm diameter photodiode with a rectangular mask over its front surface. This allowed the vertical aperture to be kept at about 8 mm so that as the detector was scanned around the silicon it did not 'walk-off' the one-dimensional diffraction pattern generated by the groove. The width of the aperture was kept in the range 2-4 mm; below 2 mm speckle noise became intrusive and above 4 mm the angular resolution was compromised, the upper size of aperture corresponding to an angular resolution of about 0.3 degrees.

The detector was scanned via an arm attached to a computer controlled rotating table, the silicon being rigidly mounted through a hole in the centre of the table. The detector signal was fed through a low-noise amplifier into a phase sensitive detector and hence into a programmable digital voltmeter and finally into the computer controlling the table rotation. Typically 1000 readings were taken in a 30° scan.

For the CO_2 measurements the He-Ne laser was replaced by a CW CO_2 laser of heavy invar construction for maximum passive stability; it produced a maximum of 3 W of TEM_{00} power on the P20 (00'1-10'0) line. A dither stabilisation scheme was incorporated into the laser to keep power fluctuations below 0.1%. A Brewster window was included in the cavity to ensure a well defined polarisation direction. The photodiode detector was replaced by a pyroelectric one. A rotatable wire grid polariser was attached to the front of the detector housing to allow the amount of depolarisation caused by the groove to be determined. The plane of polarisation of the laser radiation incident on the groove could be rotated by means of a zinc selenide half wave plate between the laser and the silicon groove.

Figure 4 shows two typical He-Ne angular scans of the mean scattered intensity $I(\theta)$ on a log-linear plot. The traces have been moved vertically to separate them and do not reflect differences in measured signals. Both traces arise from grooves having the same nominal width of 20 μm but different depths, the top one being from the $\frac{1}{4}$ hour etched

slice and the lower one from the $\frac{1}{2}$ hour one. Both traces display two obvious periods; the short 'sinusoidal-type' period can be attributed to the width of the groove and the longer period modulation to its depth.

Rather than relying on the groove widths being exactly the same as that of the mask used to make them, the width of each groove was measured using a microscope. This showed that nominally identical widths on different slices were in fact slightly different, the widths being generally wider with increasing etching time. No variation of width along a groove was apparent. Figure 5a is a plot of the measured angular positions of the minima of the diffraction pattern from the 1 hour etch slice (using He-Ne radiation) versus that predicted from (5) using the measured widths. The crosses are from the 23.5 μm wide groove (nominally 20 μm) and the circles are from the 7.3 μm (nominally 4 μm) groove. The close agreement between these results and the predicted dotted line indicates that the theory is adequate. Similar results were found for all the other grooves including the 4 μm nominal groove width, which was indeed actually 4 μm , on the $\frac{1}{2}$ hour etch slice.

The minima due to the groove depth are somewhat less well defined than those due to the width. This is principally due to non-uniformity in depth of any one groove. On any one silicon slice all the grooves and their adjacent 100 μm wide delineation grooves should all be of equal depth. The actual depth was measured using an Alpha-Step profile measuring instrument scanned across one of the delineation grooves. In general the depth varied across the groove by anything up to 1 μm . The variation is presumably less across the much narrower grooves used in the experiment. However, under a microscope various apparently random depth variations could generally be seen along any one groove. Consequently it is likely that any groove will vary in depth by a significant fraction of the visible probing wavelength over its illuminated length (20-1000 μm). Hence the diffraction minima can be expected to appear 'smoothed-out' to some degree, as found. The depth induced minima corresponding to the lower scans in Figure 4 are shown by arrows.

From plots such as those in Figure 4 the angles at which depth induced minima occurred were found by inspection. A check was made to see if successive minima were equally spaced in $\cos\theta$, and the mean depths and standard deviation calculated from (4). These calculated depths for nominally 20 μm wide grooves are shown in Figure 5b plotted against the Alpha-Step measurements. The error bars on the Alpha-Step measurements encompass the depth variation measured across the 100 μm delineation grooves. From this plot it can be seen that there is no evidence of any significant discrepancy between the depths determined using the scattering data and those measured using the profil measuring device. Similar results were found using the 4 mm grooves.

For the infrared measurements the laser radiation was focussed on to the silicon, the spot diameter being in the range 20-100 μm . A lens was also placed in front of the detector, and the detector to silicon distance was reduced to 300 mm to increase the signal to noise ratio. A Fraunhofer configuration was still however maintained. The angular distribution of scattered radiation was measured in the same plane as the incident beam, the specular direction being defined as the origin of the angular scale. A series of experiments were performed with the input radiation (electric field vector E) polarised either parallel (p) to the groove (perpendicular to the plane of incidence) or orthogonal (s) to it (in the plane of incidence ie magnetic vector H parallel to groove) as shown in Figure 6. The wire grid polariser on the front of the detector was adjusted in each case to maintain alignment with the laser polarisation direction. Because of the difficulty of ensuring that the small area detector was exactly traversing the weak one-dimensional diffraction pattern and not 'walking-off' it, the angular scans for each groove were repeated several times with the alignment being checked each time. The resultant intensity scans were normalised with respect to the measured laser power to correct for any long term laser power fluctuations. Figure 7 is a log-linear plot of the measured angular variation of the scattered intensity (normalised with respect to laser power and quoted in arbitrary units) versus angle for a groove depth of 30 μm and nominal groove

widths of 20 μm and 4 μm . The laser polarisation direction is parallel to the grooves (p) and the angle of incidence (θ_i) is approximately 8° . The bottom trace is that of the laser beam striking the flat silicon surface rather than a groove. There is more scatter in these results than in the visible laser ones due to both the poorer signal to noise ratio and the larger speckle size. Nevertheless the general features are readily apparent; at small scattering angles ($< 10^\circ$) there is a strong specular component and at larger angles the diffuse component dominates. The measured scattering from the flat silicon is less than that from even the smallest groove because it is both relatively smooth and, unlike the grooves it has a two dimensional random structure and so does not preferentially scatter radiation into the direction scanned by the detector.

To check for cross-depolarisation the wire grid polariser attached to the detector housing was set orthogonal to the input polarisation direction and angular scans performed. For all groove widths and both input polarisation directions the depolarised component, defined as the ratio of the signal measured with the polariser orthogonal to the input radiation polarisation direction, to that with it parallel was less than 5%. This is probably an upper estimate as the depolarised signal was very close to the noise threshold except near the specular direction.

From plots such as those shown in Figure 7 the scattered intensity was integrated from $\theta = 11^\circ$ to $\theta = 25^\circ$ and plotted as a function of groove width for two angles of incidence (8° and 27°) for p-polarisation in Figure 8a and s-polarisation in Figure 8b. To give an indication of the run-to-run scatter the maximum and minimum values of the integrated intensity obtained from different experimental runs are given for some values of groove width. The lower integration limit of 11° excludes specular contributions and the upper limit of 25° corresponds to the angle beyond which the poor signal to noise ratio distorts the measurements for narrow grooves. Also shown are theoretical curves calculated from (2). The depth term in this equation [$1 - \cos(2\phi_0 \cos \theta)$] only moves the calculated curve up and down the vertical axis without changing its shape. The calculations have been carried out for a groove depth of 5 μm ; small changes in this term produce large vertical movements of the curve. For groove widths less than the wavelength, the integrated intensity is proportional to s^2 . For comparison lines of slope two have been drawn through the experimental results in both Figures 8a and 8b. With the exception of the deep groove small angle of incidence case, the results are seen to be consistent with the theoretical curves, although grooves sufficiently wide to check for the roll-over in the curve were not studied. The reason for the large peak in the p-polarisation and dip in the s-polarisation results at $s \sim \lambda$ for the $d \sim 30 \mu\text{m}$, $\theta_i = 8^\circ$ case is not known.

Figure 9 shows the ratio of the integrated intensity with p-polarisation to that with s-polarisation as a function of groove width for the curves shown in Figures 8a and 8b. It can be seen that the grooves scatter the p-polarisation radiation more than the s-polarisation; the ratio rises from the a little over unity at small groove widths to a maximum around $s \sim \lambda$ and decreases slightly at larger values of s . However even when $s \sim 2\lambda$ the ratio is still of order 1.5. Scattering from the silicon away from the grooves gave a ratio of unity as expected. The unexplained resonance at $s \sim \lambda$ in the low angle of incidence, deep groove case is especially marked, and produces a very large Gaussian-type feature.

4 DISCUSSION

The elementary scalar theory outlined in section 2 is strictly only valid when the laser wavelength is small compared to the groove width. For the $\lambda = 10.6 \mu\text{m}$ experiments this condition is not satisfied and a full vector theory approach is generally thought necessary.

Although much work^(3,4,5) has been carried out for the case of a transmitting slit in a perfectly conducting screen, relatively little has been carried out for grooves in a non-perfectly conducting material. However, one relevant treatment is that of Dill and Jacobs⁽⁶⁾ who considered scattering of Ne-Ne laser radiation ($\lambda = 633 \text{ nm}$) by a rectangular groove in a conducting aluminium substrate. The groove was slightly longer than the laser wavelength and had a width to wavelength ratio of 0.8 and a depth considerably less than a wavelength (110 nm). They considered the cases of both p and s polarised light and found significant differences between the scalar and vector theory calculations. Using vector theory they showed that at the bottom of the groove close to the walls parallel to the incident E-vector the amplitude was small, whereas close to the walls perpendicular to E the amplitude was large compared to the calculated scalar value. They also found that the phase was largest, corresponding to a greater optical depth of the groove, nearer the walls perpendicular to E. These results can be qualitatively explained⁽⁶⁾ by comparing them with the solution of Sommerfeld⁽³⁾ for the problem of diffraction by a narrow slit in a perfectly conducting infinitely thin screen. Sommerfeld showed that when the incident field is p-polarised its electric field E is parallel to the walls. Since the screen is a perfect conductor the electric field must be zero inside the screen. Hence by the electromagnetic boundary condition requirement that the tangential component of the electric field is continuous across the boundary, the electric field just inside the groove must also be zero. Consequently for p-polarised radiation the groove appears narrower than its physical width. For s-polarised radiation the electric field vector is normal to the groove walls and by the continuity of the normal component of electric displacement boundary condition, the field is not zero at the boundary. Consequently radiation incident on the groove is only slightly affected by the edges and most is transmitted into the groove. Although the aluminium used by Dill and Jacobs was not assumed to be a perfect conductor, the above description explains their results in a qualitative manner. This is outlined in reference 7 as follows. When the incident radiation is p-polarised it is everywhere tangential to the conducting surface and a considerable amount of the light is reflected by the edges and walls of the groove, resulting in only small fields at the bottom near the walls. It also means that the average phase of the reflected light is smaller than predicted by scalar theory (kd) and the groove appears shallower. When s-polarised light is used little is reflected by the edges and because the electric field is discontinuous across the boundary at the walls, a large proportion of the light may reach the bottom with a relatively large amplitude and be reflected. Also the phase is larger.

From work on arrays of grooves⁽⁷⁾ similar to the single ones just described⁽⁶⁾ it is found experimentally that, as predicted, the intensities of the diffraction orders are greater by a factor of about two when the radiation is s-polarised compared to that when it is p-polarised. Also when the optical contrast between groove and surface is reduced, for example by replacing the aluminium by a dielectric, the polarisation effects became smaller. For slits in perfect conductors^(4,8) the polarisation effects are enhanced as the slit depth is increased. However the work of Dill and Jacobs⁽⁶⁾ on arrays of rectangular grooves in aluminium show that the deviation from scalar theory predictions increases as the groove width is reduced below the wavelength, but the groove depth has little effect on the relative deviation, although their results are limited to a maximum depth of $\lambda/2$.

It is difficult to reconcile the results of references 6 and 7 for a conducting surface and which predict that the scattered intensity should be greater for s-polarised radiation than p-polarised radiation with our results for a dielectric surface which show the opposite result. It should also be noted that the magnitude of the effect (a factor of order two except for the case when a large resonance occurs) is comparable. The possibility of the large resonance being due to a surface plasmon effect cannot be excluded.

The silicon targets used in this work were made of 380 μm thick n-type silicon with a doping level of $4 \times 10^{20} \text{ m}^{-3}$, corresponding to a resistivity of 13 $\Omega \text{ cm}$. The refractive index of it at 10.6 μm is 2.4 and the extinction coefficient is zero⁽⁹⁾. This high value of the refractive index may account for the ratio of the scattered intensities in

p and s polarisation being as high as those found using a good conductor in reference 6, 7. Only the front face of the silicon was polished, and had a reflectivity of 32% at 10.6 μm . The rear face was unpolished and had a rms roughness of 0.2 μm . Only the specular beam could be readily seen in transmission, scattering at the rear face making it impossible to see the weak level of radiation scattered by the grooves. This is not expected to significantly affect the results since the radiation scattered by the grooves in the forward direction, then re-scattered back through the silicon by the rear surface and thence transmitted through the front silicon face is very small compared to that backscattered by the groove.

5 CONCLUSIONS

The work described here has shown that, as expected, there is no discrepancy between the measured angular positions of the diffraction minima from a single deep phase object and those predicted using simple scalar diffraction theory when the probing wavelength is at least six times smaller than the structure. When however the laser wavelength is increased to become comparable with the structure size complex variations in the amount of scattering with polarisation direction and angle of incidence occur.

In general it is found that, contrary to expectation based on scattering from conductors, the scattered radiation from the dielectric object studied here is greater when the input radiation is p-polarised than when it is s-polarised. Apart from one particular combination of groove depth and angle of incidence where a large unexplained resonance occurs, the ratio of scattered intensities is of order two. The variation of scattered intensity with groove width for widths less than or comparable with the wavelength is consistent with a square law behaviour predicted on the basis of a simple scalar approach. To try and clarify the situation future experiments are planned with higher doping levels in silicon targets and hence higher conductivities, which will allow the target to be modelled as a good electrical conductor.

ACKNOWLEDGEMENTS

The authors are greatly indebted to Dr P H Tufton for providing the silicon groove targets and to M Dyball for carrying out the Alpha-Step measurements.

REFERENCES

- 1 D L Jordan, R C Hollins, E Jakeman; *Appl Phys B*, **31**, 179 (1983).
- 2 P Beckmann, A Spizzichino; *The Scattering of Electromagnetic Waves from Rough Surfaces* (Pergamon, 1963).
- 3 A Sommerfeld; *Optics Vol IV* (Academic Press, 1964).
- 4 S C Kashyap; *IEEE Trans Antennas and Propag*, **AP-19**, No 4, 499 (1971).
- 5 K Hongo, G Ishii; *IEEE Trans Antennas and Propag*, **AP-26**, No 3 (1978).
- 6 J G Dill, B A J Jacobs; *J Opt Soc Am*, **69**, No 7 (1979).
- 7 G Bouwhuis, J Braat, A Huijser, J Pasman, G van Rosmalen, K Schouhamer Immink; *Principles of Optical Disc Systems* (Adam Hilger, 1985).
- 8 Kh L Garb, J B Levinson, P Sh Fridberg; *Radio Eng Electron Phys*, **13**, 1888 (USSR 1968).
- 9 P J Gorton, R M Jenkins; *J Modern Optics*, **35**, No 3, 387 (1988).



FIG 1 SCATTERING GEOMETRY

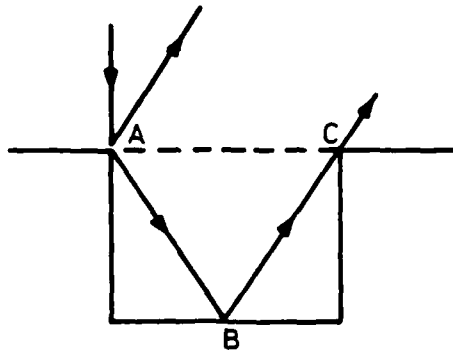


FIG 2a LIMIT OF SINGLE SCATTERING

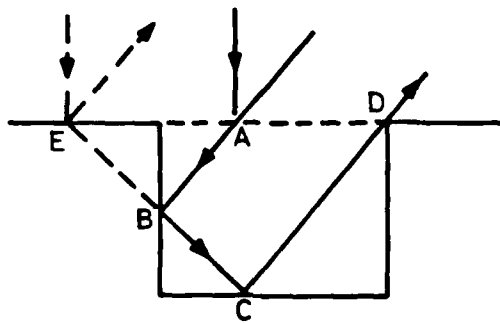


FIG 2b MULTIPLE SCATTERING

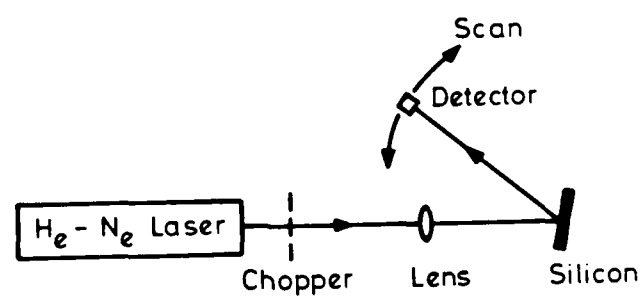


FIG 3 EXPERIMENTAL ARRANGEMENT

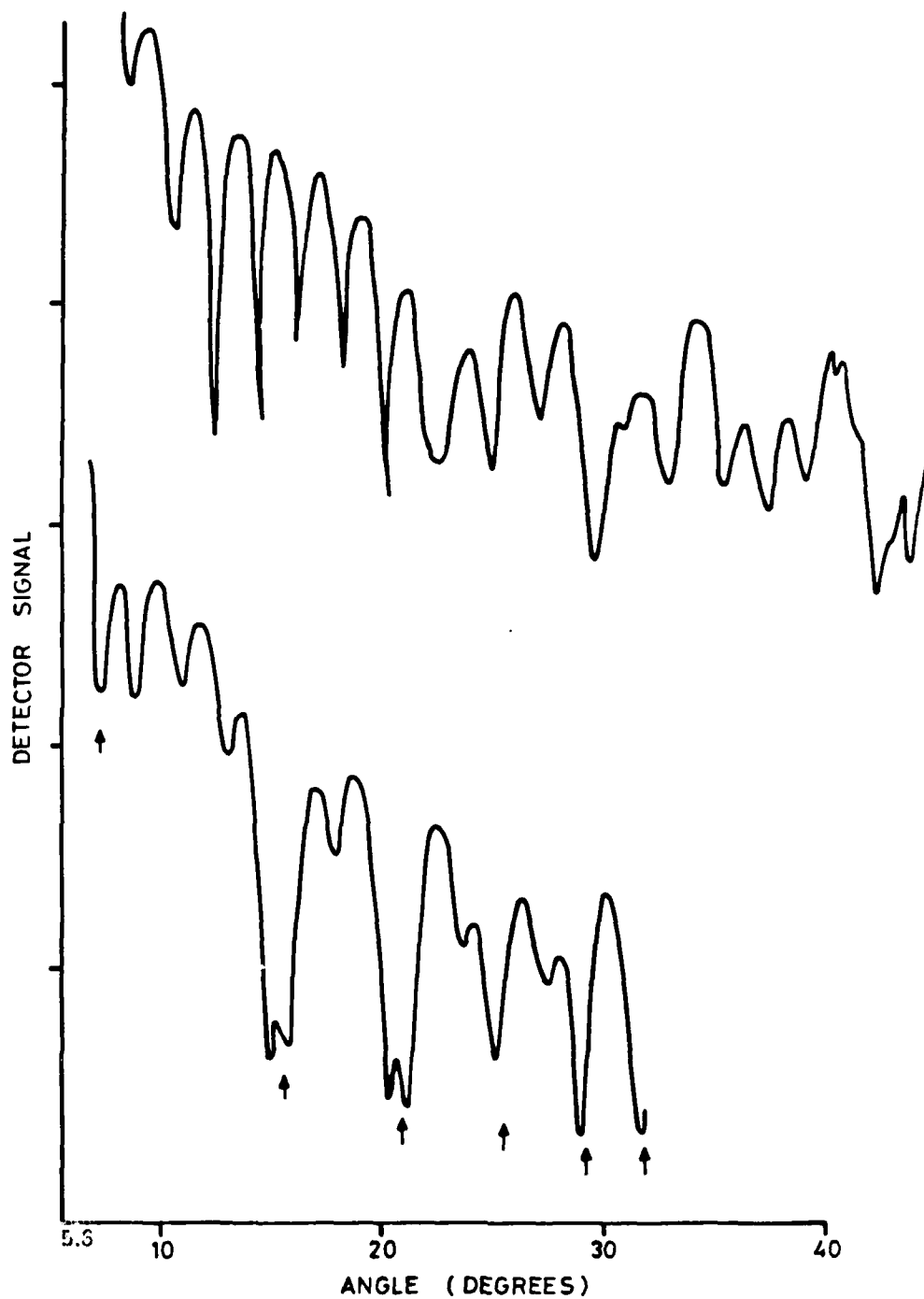


FIG 4 ANGULAR SCANS. UPPER TRACE - $\frac{1}{4}$ HOUR ETCH,
LOWER TRACE - $\frac{1}{2}$ HOUR ETCH

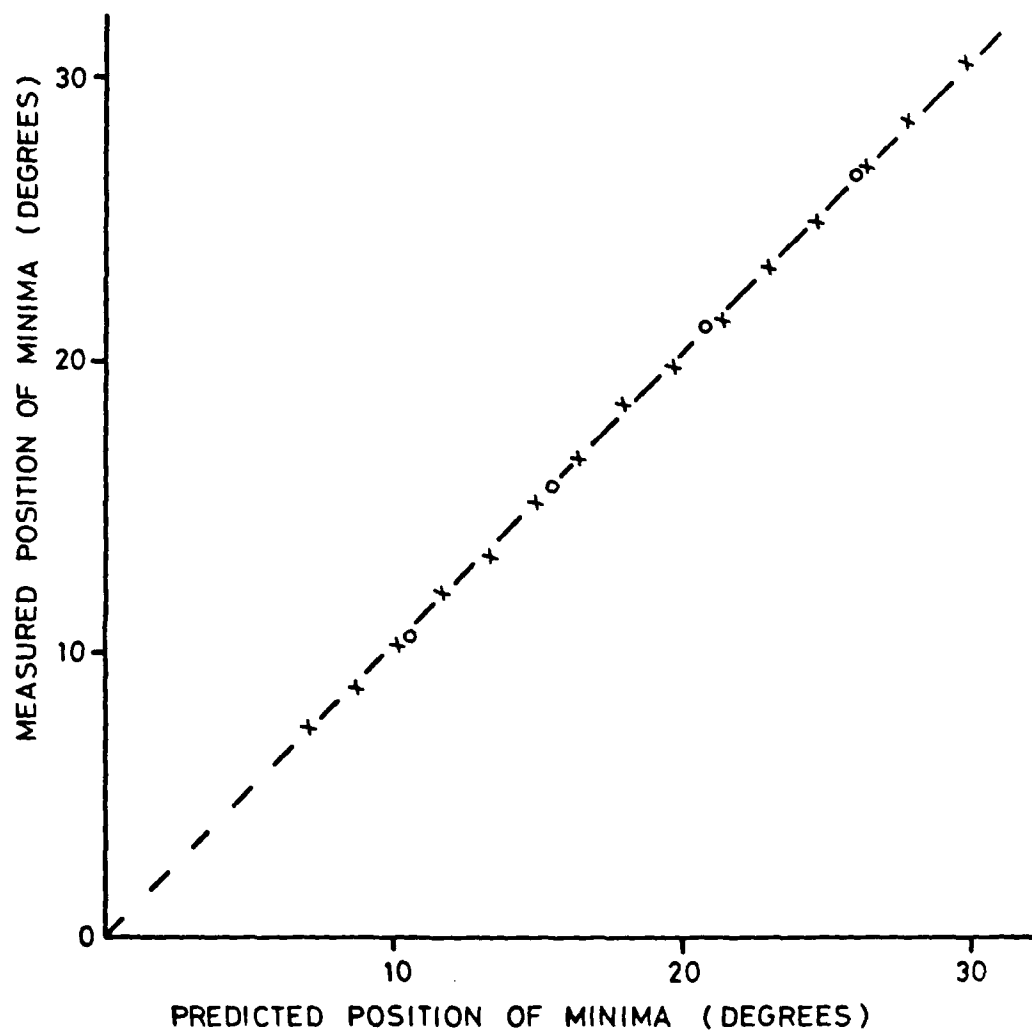


FIG 5a MEASURED VERSUS PREDICTED ANGULAR POSITIONS OF DIFFRACTION MINIMA DUE TO GROOVE WIDTH. X - 23.5 μm WIDTH GROOVE, O - 7.3 μm WIDTH GROOVE

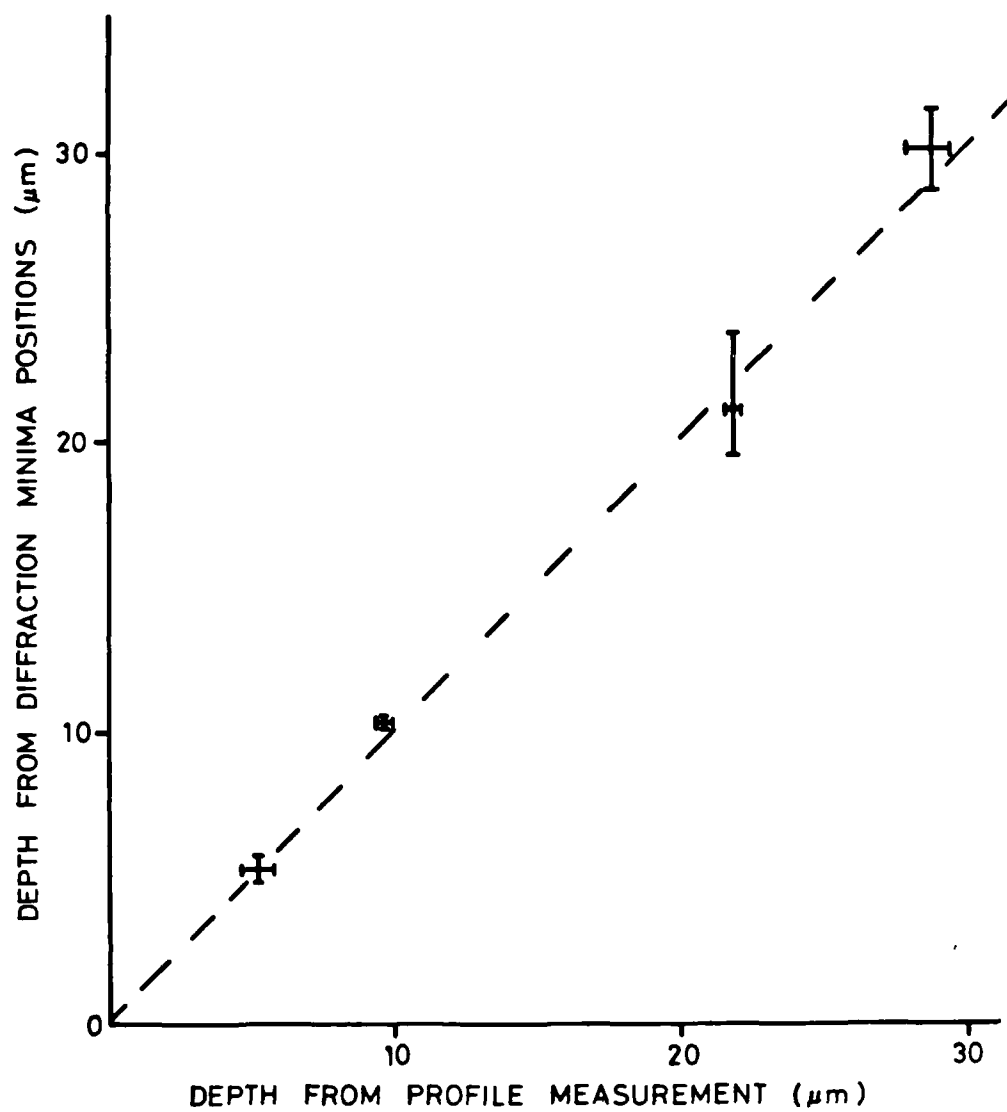


FIG 5b DEPTH OF GROOVES DETERMINED FROM DEPTH INDUCED DIFFRACTION MINIMA VERSUS THOSE DETERMINED FROM PROFILE MEASUREMENTS. NOMINAL WIDTH 20 μm

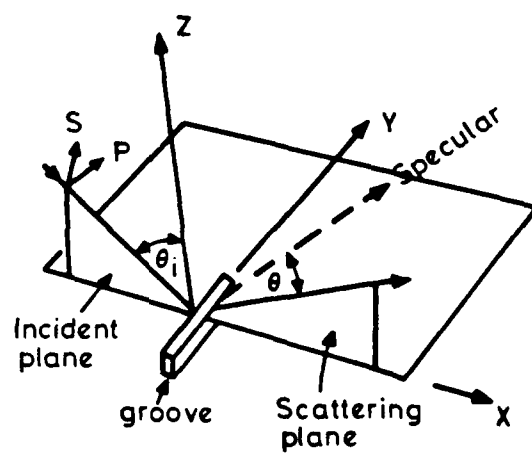


FIG 6 SCHEMATIC DIAGRAM SHOWING POLARISATION PLANES FOR INFRARED MEASUREMENTS

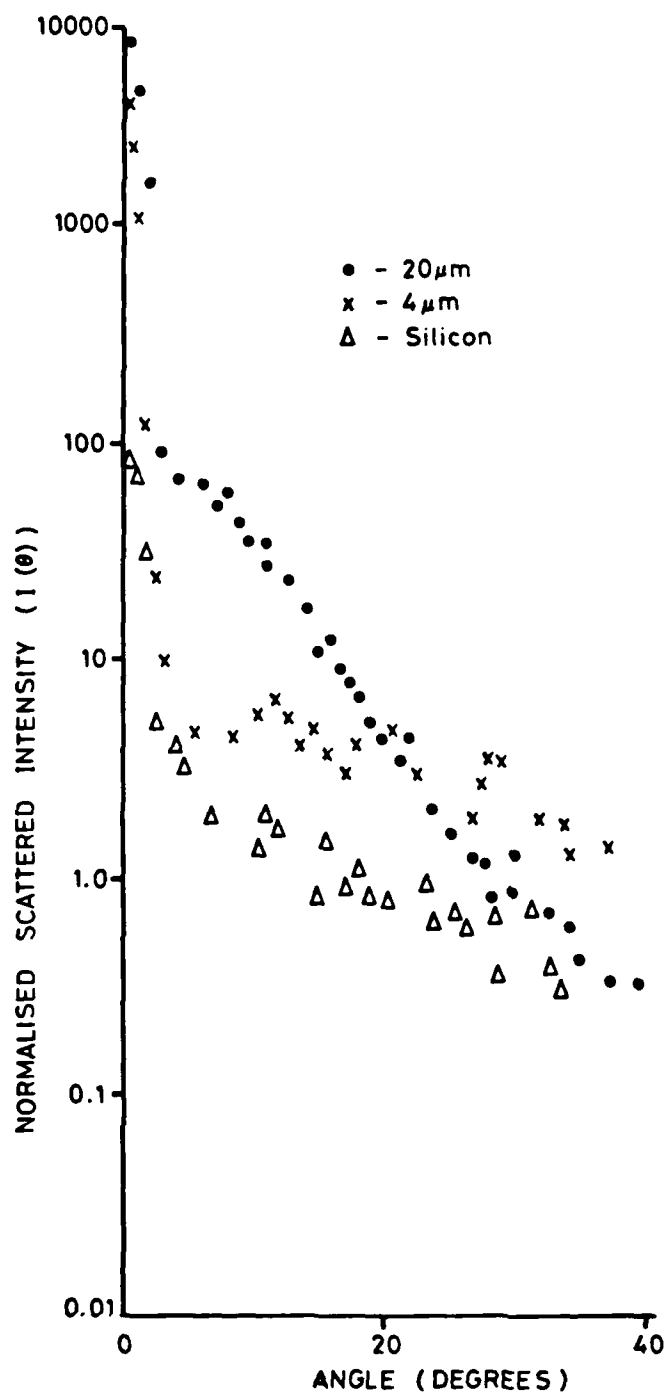


FIG 7 ANGULAR SCAN FROM 30 μ m DEEP GROOVE USING CO₂ LASER

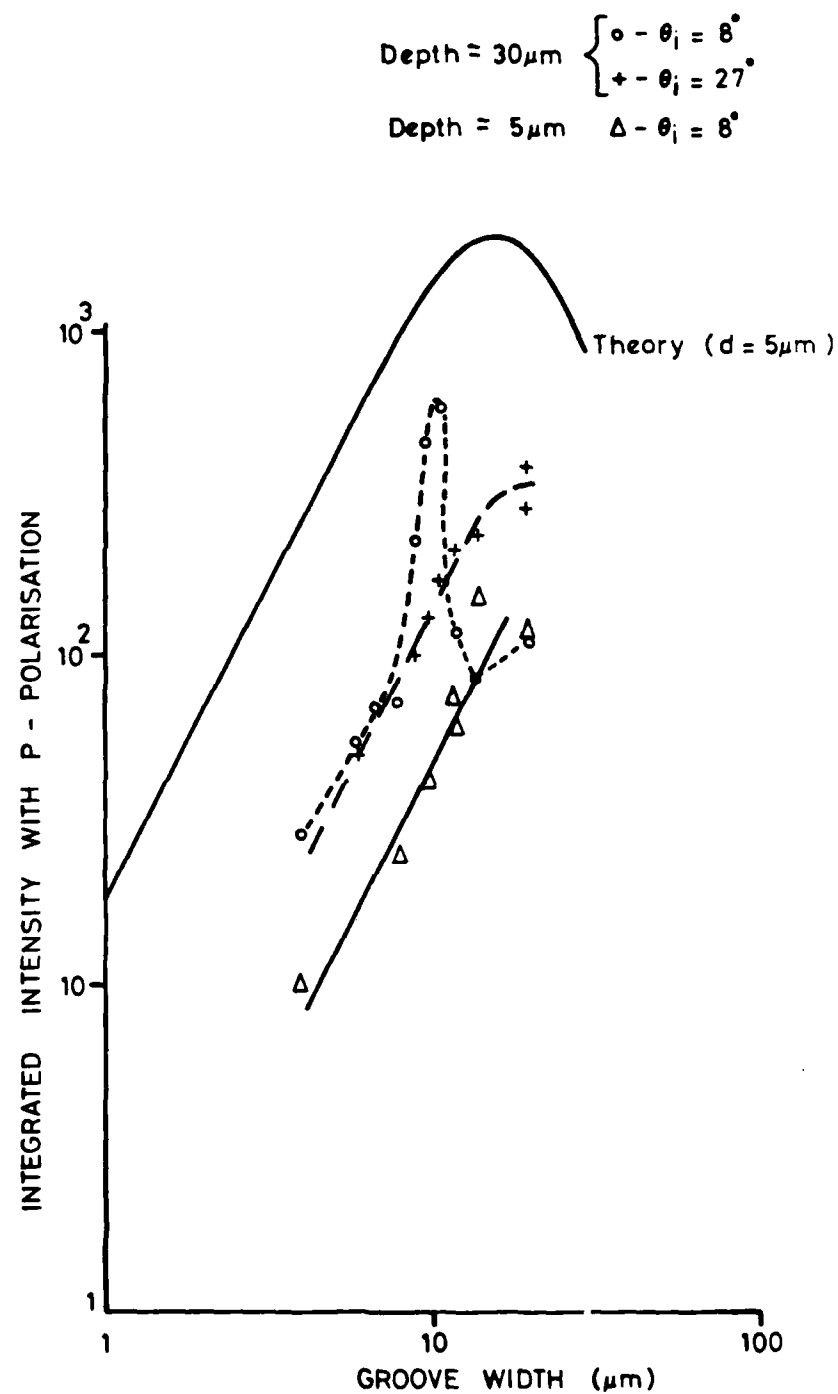


FIG 8a CO_2 INTEGRATED SCATTERING SIGNAL VERSUS GROOVE WIDTH WITH INCIDENT RADIATION p-POLARISED

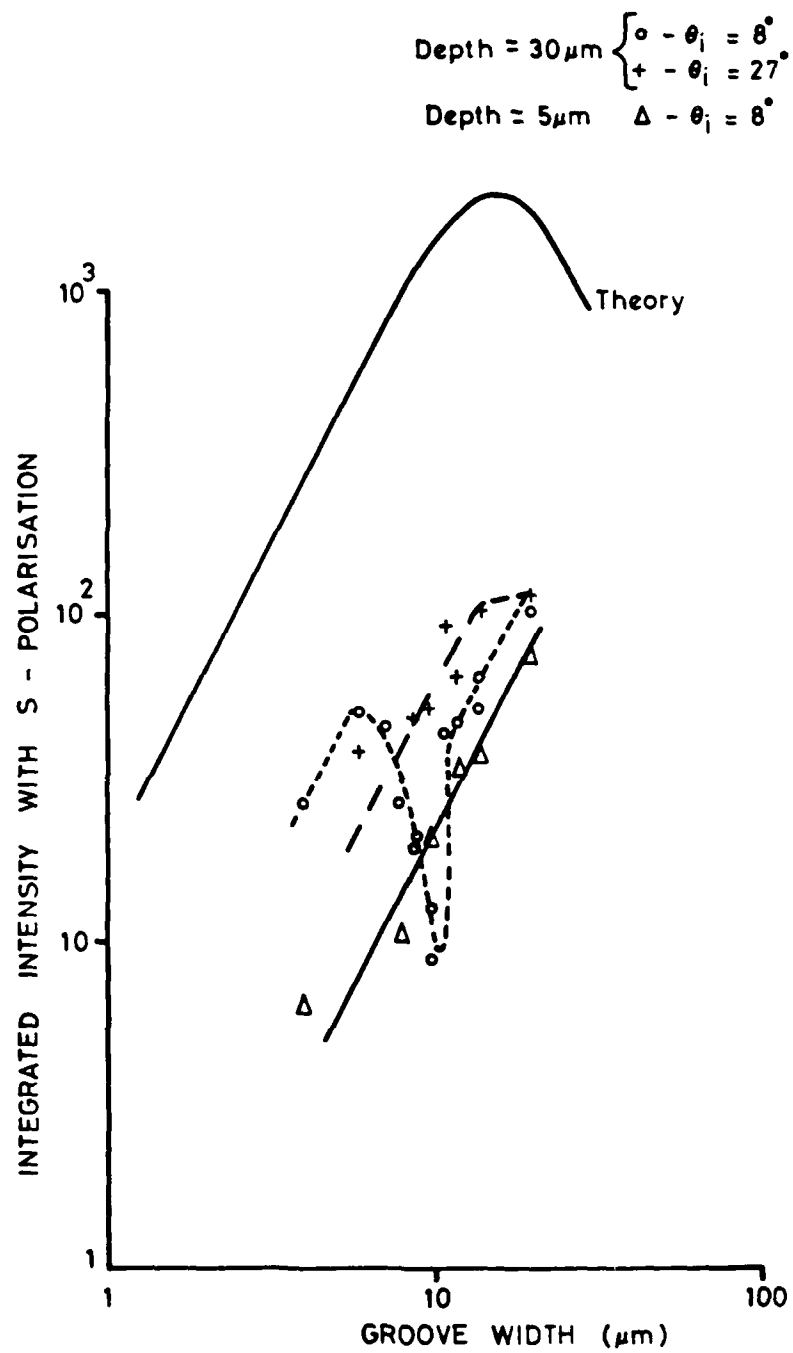


FIG 8b CO₂ INTEGRATED SCATTERING SIGNAL VERSUS GROOVE WIDTH WITH INCIDENT RADIATION s-POLARISED

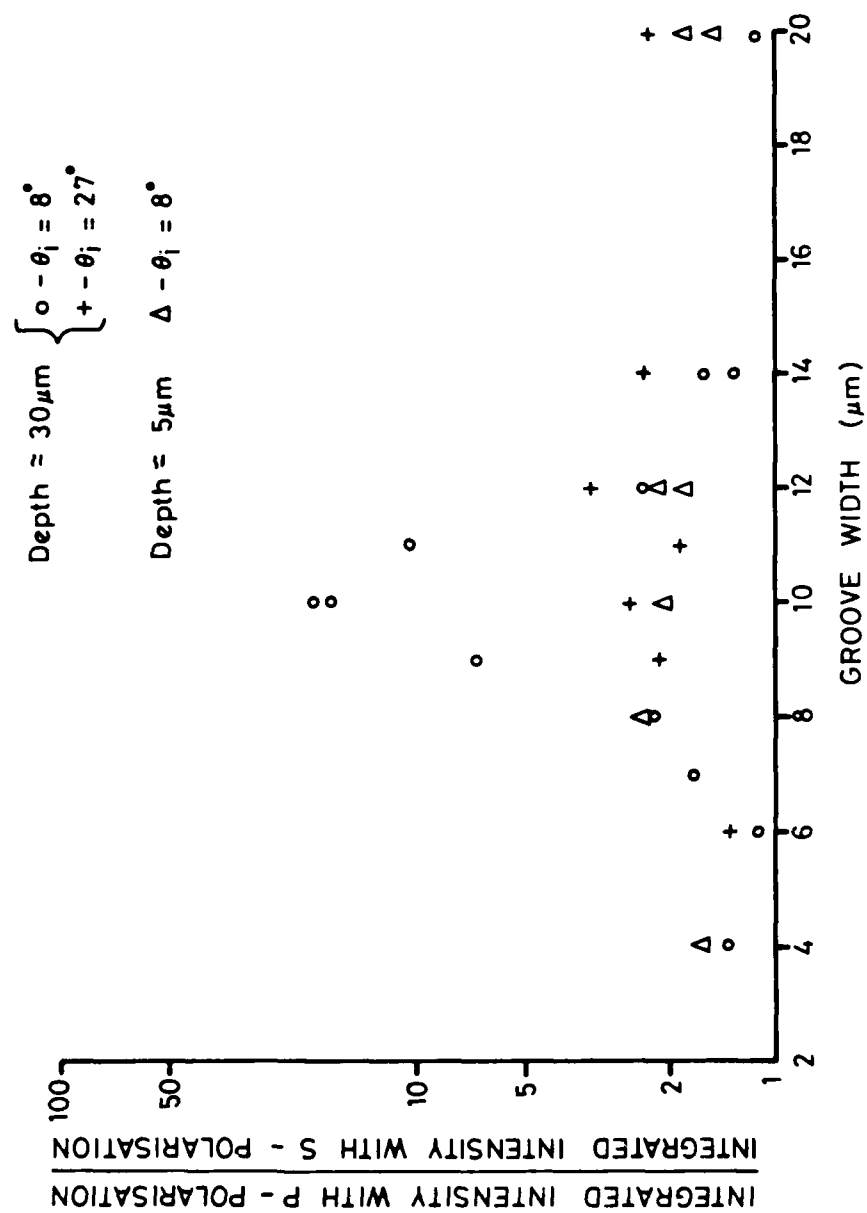


FIG 9 RATIO OF CO_2 INTEGRATED INTENSITY WITH INCIDENT RADIATION
 p-POLARISED TO THAT WITH IT s-POLARISED AS A FUNCTION OF
 GROOVE WIDTH

DOCUMENT CONTROL SHEET

Overall security classification of sheet ...UNCLASSIFIED.....

(As far as possible this sheet should contain only unclassified information. If it is necessary to enter classified information, the box concerned must be marked to indicate the classification eg (R) (C) or (S))

1. DRIC Reference (if known)	2. Originator's Reference Memorandum 4191	3. Agency Reference	4. Report Security Classification Unclassified	
5. Originator's Code (if known) 7784000	6. Originator (Corporate Author) Name and Location Royal Signals and Radar Establishment St Andrews Road, Malvern, Worcestershire WR14 3PS			
5a. Sponsoring Agency's Code (if known)	6a. Sponsoring Agency (Contract Authority) Name and Location			
7. Title EXPERIMENTAL MEASUREMENTS OF SCATTERING FROM SIMPLE WAVELENGTH SIZED PHASE OBJECTS				
7a. Title in Foreign Language (in the case of translations)				
7b. Presented at (for conference papers) Title, place and date of conference				
8. Author 1 Surname, initials Jordan D L	9(a) Author 2 Jakeman E	9(c) Authors 3,4... Hollins R C	10. Date 8.88	or ref. vp
11. Contract Number	12. Period	13. Project	14. Other Reference	
15. Distribution statement Unlimited				
Descriptors (or keywords)				
continue on separate piece of paper				
<p>Abstract</p> <p>Experimental results are presented for the angular distribution of radiation scattered from single deep grooves etched in silicon. Both visible and infrared radiation is used. Whereas the grooves are wide compared to the wavelength of the visible radiation, they span a range of sizes from approximately twice down to half the infrared wavelength.</p> <p style="text-align: right;">(GAE) 4191-7</p>				